Hydrogen diffusion in acceptor-doped silicon carbide: Implementation of the reaction zone concept

M. Sinder, Z. Burshtein, and J. Pelleg
Department of Materials Engineering, Ben-Gurion University of the Negev, P.O. Box 653, Beer-Sheva 84105, Israel
(Received 2 July 2007; published 25 March 2008)

In the work of Janson *et al.* [Phys. Rev. B **64**, 195202 (2001)], an experimental study of deuterium (^{2}H) diffusion in B- and Al-doped silicon carbide (SiC) was performed. A trap-limited diffusion model was used as a basis for analysis. Using the same model, in this paper, we introduce the concept of a dynamical reaction front, namely, a distinctive, well-defined zone, to which the reaction of the deuterium-dopant complex formation is confined. This zone lies between the already-deuterated and the non-deuterated regions and penetrates gradually into the specimen. We obtain analytical expressions for the spatial profiles of the free and complexed deuterium and for the reaction rate profiles. The analysis predicts that the reaction zone width initially remains constant as the zone progresses into the sample; yet, after a certain time, the zone starts to widen proportionally to the square root of time. We propose an alternative method of experimental analysis, where the reaction zone position and width as functions of time are measured. This should yield the same process parameters, as determined by the method of Janson *et al.* [Phys. Rev. B **64**, 195202 (2001)].

DOI: 10.1103/PhysRevB.77.094128 PACS number(s): 66.30.J−, 61.72.S−, 85.40.Ry

I. INTRODUCTION

Chemical diffusion in solids is a subject of theoretical as well as practical importance.[1–4] Specifically, hydrogen diffusion in semiconductors is of interest for the purpose of acceptor passivation. Recently, Janson *et al.*[5] studied the diffusion kinetics of deuterium (^{2}H) in acceptor-doped silicon carbide (SiC). The acceptors used were boron (B) and aluminum (Al). The aim was to establish the diffusion kinetic parameters and to accurately determine the dissociation energies of the ^{2}H-B and ^{2}H-Al complexes. ^{2}H was introduced using ion implantation and the ^{2}H depth profiles were determined by secondary ion mass spectrometry (SIMS). The theory of trap-limited diffusion was used to extract the process parameters from the experimental data. Janson *et al.*[5] found out that in the high dissociation regime, the ^{2}H diffusion is controlled by an effective diffusion coefficient that is entirely determined by the trapping-dissociation process of the ^{2}H/acceptor complex and is independent of the ^{2}H diffusion constant. Thus, the experimental results in this regime would not allow determining the ^{2}H diffusion coefficient unless the concentration of free ^{2}H was known. The results, however, allowed determining the dissociation frequency of the ^{2}H/acceptor complex. In the negligible dissociation regime, usually established at sufficiently low temperatures, the experimental results allowed determining the effective capture radius of the trap (acceptor).

The experimental results as well as numerical simulations performed by Janson *et al.*[5] reveal that under certain conditions in the course of diffusion, a fall in ^{2}H concentration occurs over a short distance. This suggests the introduction of the reaction front concept for describing the penetration dynamics of ^{2}H into the SiC. The concept of a reaction front formed between initially separated reactants is used for the description of many systems in physics, chemistry, biology, geology, as well as materials science.[6,7] Gálfi and Rácz[8] addressed the problem of an irreversible reaction between the two reactants by assuming that the local reaction rate at long times $R(x,t)$ takes a scaling form $\sim t^{\alpha}\mathbf{F}[(x-x_f(t))/w(t)]$, where x is the position, t is the time, and $x_f(t)\sim t^{\beta}$ and $w(t)\sim t^{\gamma}$ are the time-dependent reaction rate peak position and reaction zone width, respectively. $\mathbf{F}$ is a scaling function. The authors obtained $\alpha=-2/3$, $\beta=1/2$, and $\gamma=1/6$ when both reactants are mobile. It has been later established[9–23] that α, β, and γ depend on some details of the process: specifically, the dimensionality of the space where diffusion occurs,[9–14] mobility or immobility of one of the reactants,[15,16] and reversibility or irreversibility of the reaction.[17–23] Their seminal work was followed theoretically and experimentally by many authors.[24–45] Koza[16,27] has carried out a systematic analysis of the irreversible reaction case for arbitrary values of the diffusion constants and of the initial concentrations of the reactants, including the case where one of the reactants is static.[16] In his work, he presents differential equations for scaling functions used in the theory for the latter case. Several authors[17–23] extended the study of reaction-diffusion systems to reversible reactions. In particular, Sinder and Pelleg[18–20] introduced a single iteration of the steady state solution as a method for calculating the reaction rate profiles, thus showing that the concept of a reaction front may be applied to reversible reaction-diffusion systems as well. Koza[21–23] then developed a new technique for studying (analytically and numerically) reversible reaction-diffusion systems of arbitrary nature by expansion of the reactants' and reaction product concentrations as power series in $1/t$.

In our present work, we extend the theory presented by Janson *et al.*[5] by applying the reaction front concept to the same physical system. We present analytical solutions to the hydrogen time-dependent spatial profiles applicable to both irreversible and reversible reaction regimes. The general solution reveals effects concerning the time dependence of the reaction zone width. We propose a fresh approach to the analysis of experimental results, which is based on the effects. We show that it allows obtaining the diffusion parameters in a straightforward and coherent manner.

II. MODEL

We present briefly the model used by Janson *et al.*[5] A diffusing mobile reagent A (specifically hydrogen ^{2}H) reacts with an immobile trap T (boron or aluminum acceptors) to produce an immobile complex AT (hydrogen/boron or hydrogen/aluminum pairs, respectively): $A+T \leftrightarrow AT$. The process dynamics is given by

$$\frac{\partial[A]}{\partial t} = D\frac{\partial^2[A]}{\partial x^2} - \frac{\partial[AT]}{\partial t},$$

$$\frac{\partial[AT]}{\partial t} = k[A][T] - \nu[AT],$$

$$[T] = T_{\text{init}} - [AT], \tag{1}$$

where k and ν are the complex formation constant and its dissociation frequency, respectively, D is A's diffusivity, and T_{init} is the initial trap concentration. The initial conditions are $[A]_{t=0}=0$, $[T]_{t=0}=T_{\text{init}}$, and $[AT]_{t=0}=0$, with the boundary condition $[A]_{x=0}=A_0$ at all times. For simplicity, one assumes that $A_0 \ll T_{\text{init}}$.

Janson *et al.*[5] solved these equations by assuming that "the region of the diffusion front acts as a sink for the A's." This approach is equivalent to describing the system as having an infinitely thin reaction zone. This is a very popular approach used in various areas of research for many years.[46–50] Formally, it is equivalent to considering a case where the complex dissociation characteristic time ν^{-1} is very long compared to its formation characteristic time $(kA_0)^{-1}$, namely, $(kA_0)^{-1} \ll \nu^{-1}$ or, alternatively, $A_0k/\nu \gg 1$. One then solves the equations for sufficiently long times $t \gg (kA_0)^{-1}$, i.e., when the complex formation reaction overrides the dissociation.[6–8,15,16,29] An approximate solution yields $[AT]=T_{\text{init}}$, $[T]=0$, and $[A]=A_0[1-x/x_f(t)]$ for $x < x_f(t)$, and $[AT]=0$ and $[T]=T_{\text{init}}$, $[A]=0$ for $x > x_f(t)$, where the reaction front position $x_f(t)$ is given by

$$x_f(t) = \sqrt{2A_0Dt/T_{\text{init}}}. \tag{2}$$

In contrast to Janson *et al.*,[5] we assume that the reaction occurs in a region of finite width. This approach enables us to obtain a deeper insight into the process. In particular, the analysis provides expressions for the reaction rate profiles and spatial profiles of the mobile and postreacted (trapped) species. Under a broad range of conditions, the diffusion is accompanied by an irreversible reaction at sufficiently short times and transforms into a reversible one after a characteristic time t^*. The reaction zone width is constant for short times compared to t^* but turns proportional to $\sqrt{t}$ for long times compared to t^*. We propose a fresh method of experimental analysis of studying the zone width as a function of time. This should yield the relevant diffusion and reaction parameters.

III. IRREVERSIBLE COMPLEX FORMATION

The term "irreversible" relates to the case where the dissociation reaction is negligibly small compared to the complex formation reaction. This case is termed "negligible dissociation regime" by Janson *et al.*[5] It occurs in the time regime $t \gg 1/(kA_0)$ [As will be shown later, another condition is also required: $t \ll t^* = \frac{2}{9}\nu^{-1}(kA_0/\nu)$; the formal definition and physical significance of the characteristic time t^* will be given in Sec. IV, Eq. (12), and the related text.] Adopting the same approach as in Ref. 16, long-time asymptotic expressions of the component concentration profiles and of the reaction rate in the vicinity of $x \sim x_f(t)$ may be calculated. The solution is given in a parametric form. One defines the following scaling functions of the free parameter $-1 < p < 0$:

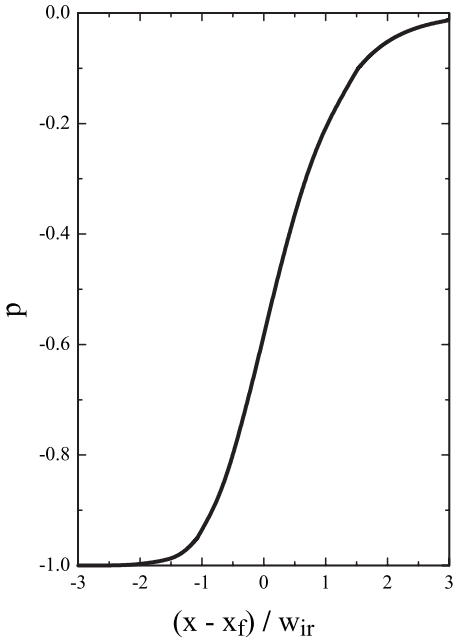

FIG. 1. Shape of function $p[(x-x_f)/w_{\text{ir}}]$ defined by Eq. (3).

$$S_A(p) \equiv \frac{\sqrt{2}}{1.47}\sqrt{p - \ln(p+1)}, \tag{3}$$

$$S_T(p) \equiv p + 1, \tag{4}$$

$$S_{AT}(p) \equiv -p, \tag{5}$$

$$S_{\mathbf{R}}(p) \equiv S_A(p)S_T(p), \tag{6}$$

and $x \equiv x(p)$ and its inverse $p \equiv p[(x-x_f)/w_{\text{ir}}]$ by

$$\frac{x - x_f}{w_{\text{ir}}} \equiv \frac{1}{1.47\sqrt{2}}\int_{-0.5828}^{p} \frac{du}{(u+1)\sqrt{u - \ln(u+1)}}, \tag{7}$$

where $w_{\text{ir}} \equiv 1.47\sqrt{D/kT_{\text{init}}}$ is the reaction zone width in the irreversible case. A formal definition of the width parameter is provided in the Appendix. The constant 1.47 in Eq. (7) is a numerical scaling factor that was determined by Koza.[16] The lower limit −0.5828 of the integral in Eq. (7) is the numerical solution for the p parameter that provides a peak in the $S_{\mathbf{R}}(p)$ scaling function [Eq. (6)] at the point $x=x_f$. Figure 1 illustrates the shape of the $p[(x-x_f)/w_{\text{ir}}]$ function.

Using the above definitions, one obtains

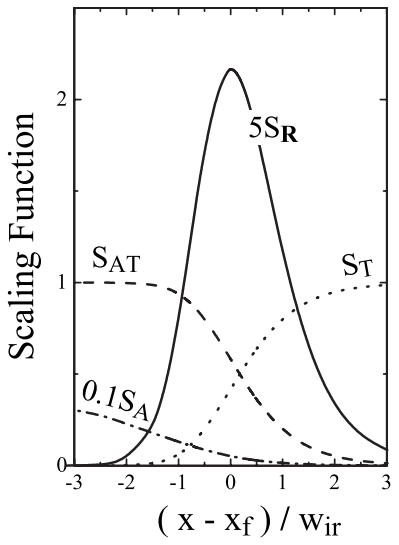

FIG. 2. Scaling functions S_A, S_T, S_{AT}, and $S_{\mathbf{R}}$ relating to the $[A]$, $[T]$, and $[AT]$ component profiles and to the reaction rate profile $\mathbf{R}$, respectively, in the irreversible reaction regime in the vicinity of the reaction front. Note that $S_{AT}=-p$ [Eq. (5)], which is just the same as $p[(x-x_f)/w_{\mathrm{ir}}]$ shown in Fig. 1, with an opposite sign.

$$\mathbf{R} = \frac{v_f T_{\mathrm{init}}}{w_{\mathrm{ir}}} S_{\mathbf{R}}\left[p\left(\frac{x-x_f}{w_{\mathrm{ir}}}\right)\right], \tag{8}$$

$$[A] = \frac{v_f T_{\mathrm{init}} w_{\mathrm{ir}}}{D} S_A\left[p\left(\frac{x-x_f}{w_{\mathrm{ir}}}\right)\right], \tag{9}$$

$$[T] = T_{\mathrm{init}} S_T\left[p\left(\frac{x-x_f}{w_{\mathrm{ir}}}\right)\right], \tag{10}$$

$$[AT] = T_{\mathrm{init}} S_{AT}\left[p\left(\frac{x-x_f}{w_{\mathrm{ir}}}\right)\right], \tag{11}$$

where $v_f \equiv dx_f/dt$ is the velocity of the reaction front position. One should note that $\mathbf{R}$, $[A]$, $[T]$, and $[AT]$ are directly proportional to their corresponding scaling functions $S_{\mathbf{R}}$, S_A, S_T, and S_{AT}.

In Fig. 2, we plotted the scaling functions defined in Eqs. (3)–(6) versus the reduced distance from the reaction front position $(x-x_f)/w_{\mathrm{ir}}$. The mobile reagent concentration $[A]$ reduces from left to right toward the reaction front position, turning virtually zero for $(x-x_f)/w_{\mathrm{ir}} \gtrsim 2$; simultaneously, the immobile trap concentration $[T]$ has been reduced to virtually zero below about $(x-x_f)/w_{\mathrm{ir}} \lesssim -2$, while maintaining its original value above $(x-x_f)/w_{\mathrm{ir}} \gtrsim 2$. The reaction product concentration [AT] exhibits a saturation value below about $(x-x_f)/w_{\mathrm{ir}} \lesssim -2$. It then reduces from left to right toward the reaction front position, turning virtually zero for $(x-x_f)/w_{\mathrm{ir}} \gtrsim 2$. The reaction rate profile exhibits a peak at the reaction front position $(x-x_f)/w_{\mathrm{ir}} \equiv 0$, with a peak width [full width at half maximum (FWHM)] of approximately 2. One may note that the condition we have set, $t \gg 1/(kA_0)$, also implies that the reaction zone width is always very narrow compared to the reaction zone distance from the surface, i.e., $w_{\mathrm{ir}} \ll x_f$.

In the Appendix, we present some asymptotic expressions for the scaling functions at large distance from the reaction zone.

IV. REVERSIBLE COMPLEX FORMATION: ASYMPTOTIC SOLUTION FOR A "NARROW" REACTION ZONE

We use the term "reversible" for the case where the net rate between the complex formation and dissociation reactions is negligibly small. Quasiequilibrium conditions require near equality of the forward $k[A][T]$ and backward $\nu[AT]$ reaction rates; it is usually achieved at sufficiently long times past the start of diffusion. An assessment of a "sufficiently long time" is based on the condition that the difference between the complex formation and the dissociation rates $\mathbf{R}(x,t) = \partial[AT]/\partial t$ is small compared to both $k[A][T]$ and $\nu[AT]$, namely, $\mathbf{R}(x,t) \ll k[A][T] \cong \nu[AT]$. Let us now define a characteristic time t^* by the equation

$$\mathbf{R}(x,t^*) = \nu[AT](x,t^*). \tag{12}$$

In principle, the solution provides a function $t^* = t^*(x)$; for simplicity, we take as a representative t^* the value $t^*(x_f)$. Quasi-steady-state conditions thus require that $t \gg t^*$. In other words, t^* characterizes the crossover between reversible (which is, in fact, quasireversible) and irreversible regimes. Using the t^* term, $t \ll t^*$ in the irreversible regime, and the backward reaction $A+T \leftarrow AT$ is negligible. In Sec. V, we show that $t^* \equiv \frac{2}{9}\nu^{-1}(kA_0/\nu)$ for our model.

Under conditions where $t \gg t^*$, one may adopt the approach described in Ref. 20, which provides asymptotic expressions for the component concentration profiles and for the reaction rate profiles in the vicinity of $x_f(t)$. One obtains the reversible reaction front width as $w_r = (\nu/k)\sqrt{2Dt/A_0 T_{\mathrm{init}}}$ per definition in the Appendix. One also defines scaling functions Q_A, Q_T, Q_{AT}, and $Q_{\mathbf{R}}$ as follows:

$$Q_A + \ln Q_A + (\ln 2 - 0.5) = -(x-x_f)/w_r, \tag{13}$$

$$Q_T = (1+Q_A)^{-1}, \tag{14}$$

$$Q_{AT} = Q_A/(1+Q_A), \tag{15}$$

$$Q_{\mathbf{R}} = Q_A/(1+Q_A)^3. \tag{16}$$

Using these definitions, one obtains

$$\mathbf{R} = \frac{T_{\mathrm{init}}}{2t}\frac{A_0 k}{\nu} Q_{\mathbf{R}}\left(\frac{x-x_f}{w_r}\right), \tag{17}$$

$$[A] = \frac{\nu}{k} Q_A\left(\frac{x-x_f}{w_r}\right), \tag{18}$$

$$[T] = T_{\mathrm{init}} Q_T\left(\frac{x-x_f}{w_r}\right), \tag{19}$$

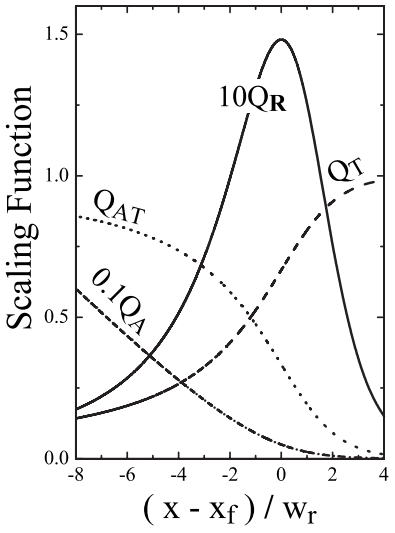

FIG. 3. Scaling functions Q_A, Q_T, Q_{AT}, and $Q_{\mathbf{R}}$ relating to the $[A]$, $[T]$, and $[AT]$ component profiles and to the reaction rate profile **R**, respectively, in the reversible reaction regime in the vicinity of the reaction front.

$$[AT] = T_{\text{init}} Q_{AT}\left(\frac{x - x_f}{w_r}\right). \tag{20}$$

Note that **R**, $[A]$, $[T]$, and $[AT]$ of Eqs. (17)–(20) are directly proportional to their corresponding scaling functions $Q_{\mathbf{R}}$, Q_A, Q, and Q_{AT} of Eqs. (13)–(16). We present some asymptotic behaviors of these scaling functions in the Appendix.

In Fig. 3, we plotted the scaling functions defined in Eqs. (13)–(16) versus the reduced distance from the reaction front position $(x-x_f)/w_r$ in a manner similar to the irreversible case of Fig. 2. The mobile reagent concentration $[A]$ reduces from left to right toward the reaction front position, turning virtually zero for $(x-x_f)/w_r \gtrsim 2$; simultaneously, the immobile trap concentration $[T]$ maintains its original value above $(x-x_f)/w_r \gtrsim 4$ while reducing asymptotically toward zero from right to left below about $(x-x_f)/w_r \lesssim -8$. The complex concentration $[AT]$ exhibits saturation below $(x-x_f)/w_r \lesssim -8$. It then reduces from left to right toward the reaction front position, turning virtually zero for $(x-x_f)/w_r \gtrsim 4$. The reaction rate profile exhibits a peak at the reaction front position $(x-x_f)/w_r=0$, with a peak width (FWHM) of approximately 5.

In summarizing the physical conclusions of the theory, a striking effect is seen.

It concerns the reaction zone-width parameter w as a function of time (see Appendix). At times shorter than t^*, w is given by $w \cong w_{\text{ir}} \equiv 1.47\sqrt{D/kT_{\text{init}}}$ [see text following Eq. (7)]. For long times compared to t^*, $w \cong w_r \equiv (\nu/k)\sqrt{2Dt/A_0 T_{\text{init}}}$ [see text preceding Eq. (13)]. Summarizing,

$$w = \begin{cases} 1.47\sqrt{D/kT_{\text{init}}} & \text{for } t \ll t^* \\ [(\nu/k)\sqrt{2D/A_0 T_{\text{init}}}]\sqrt{t} & \text{for } t \gg t^*. \end{cases} \tag{21}$$

In other words, the reaction zone width remains constant at times much shorter than t^* and grows linearly as a function of $\sqrt{t}$ for times much longer than t^*. Such an effect is useful for the analysis of experimental results. One should plot the reaction front width as a function of $\sqrt{t}$ and establish the constant short-time width $w(0)=1.47\sqrt{D/kT_{\text{init}}}$ and the point where the width starts to rise: $t^*=\frac{2}{9}\nu^{-1}(kA_0/\nu)$. One expects this point to be established fairly accurately by plotting a horizontal line that fits the points in the short $\sqrt{t}$ and a straight line intersecting the origin that fits the points in the long $\sqrt{t}$. One should then analyze a plot of the reaction front position x_f as a function of $\sqrt{t}$, whose slope is slope $=\sqrt{2A_0 D/T_{\text{init}}}$ [Eq. (2)]. Solving for the physical diffusion parameters, one obtains

$$\nu = 0.4 \cdot \text{slope}/w(0)\sqrt{t^*},$$

$$DA_0 = 0.5T_{\text{init}} \cdot \text{slope}^2,$$

$$k/D = 1.47/T_{\text{init}} \cdot w(0)^2. \tag{22}$$

This is the same list of process parameters obtained by Janson *et al.*[5] using a different method of analysis. Unfortunately, we are unable now to demonstrate the use of our proposed method on the basis of their available experimental data. The annealing time required to take advantage of the proposed method is naturally longer than usually used for diffusion analysis experiments. The process parameters obtained by Janson *et al.*[5] for their lower annealing temperature (470 °C) were $A_0 \approx 10^{14}$ cm^{-3}, $\nu=1.2\times10^{-4}$ s^{-1}, and $k \cong 5 \times 10^{-17}$ cm^{-3}. One then estimates $t^* \cong 10$ h. Observation and analysis of the reaction zone broadening would require annealing durations of approximately ~100 h — a reasonable figure from an experimental point of view.

To complete this section, we propose a method for conveniently identifying the width parameter w and reaction front position x_f from a measurement of the $[AT]$ profile. One should simply fit the profile to an empiric function of the form

$$[AT](x) = \frac{T_{\text{init}}}{1 + \exp[(x - x_f)/w]}, \tag{23}$$

with T_{init}, x_f, and w acting as free parameters. We have established that the fit parameters differ from those obtained by the exact analytical expressions [Eqs. (7) and (11) for the irreversible case and Eqs. (13), (16), and (17) for the reversible case] by only a few percent. Furthermore, the use of the exact equations for fitting is limited to the short annealing time end [Eqs. (7) and (11)] or to the very long annealing time end [Eqs. (13), (16), and (17)] but not in the intermediate. On the other hand, Eq. (23) may be equally used for fitting throughout the entire annealing time range. A demonstration of the closeness between the "empiric" fit using Eq. (23) and the accurate fit, for an irreversible reaction case, will be provided in Sec. VI.

Standard experimental procedures for studying diffusing species concentrations often involve SIMS. In our case, the measurements would thus resolve the sum $[AT]+[A]$, rather than just that of $[AT]$, as required by Eq. (23). However, the exact solutions for our case show that the condition $[AT] \gg [A]$ is always satisfied, in the irreversible as well as in the

reversible case. Formally, it follows from the basic conditions underlying our analysis: $A_0 \ll T_{\text{init}}$ and $A_0 k/\nu \gg 1$. From an experimental point of view, if a steep change in the measured SIMS signal is observed, the apparent width parameter is obviously narrow compared to the distance from the surface. One may then safely assume the validity of the condition $[AT] \gg [A]$ and take advantage of Eq. (23).

V. REVERSIBLE COMPLEX FORMATION: ANALYTIC SOLUTION

In the work of Janson *et al.*,[5] an analytic solution for quasiequilibrium conditions based on an effective diffusion coefficient approach is presented and used for the limit $A_0 k/\nu \ll 1$. Here, we grossly relax that limit. We show that as long as $A_0 k/\nu + 1 \ll \sqrt{T_{\text{init}}/k\nu}$, an analytical solution may exist even for $A_0 k/\nu \gg 1$ (see Appendix). Note that once $A_0 k/\nu \ll 1$, one may rewrite the above condition as $1 \ll \sqrt{T_{\text{init}} k/\nu}$; once $A_0 k/\nu \gg 1$, one may rewrite that condition as $A_0 k/\nu \ll T_{\text{init}}/A_0$. In some experiments described in Ref. 5, it has been estimated that $A_0 \approx 10^{14}$ cm^{-3} and $T_{\text{init}} \approx 10^{17}$ cm^{-3} (for example, Figs. 5 and 6 in Ref. 5); thus, $T_{\text{init}}/A_0 \sim 10^3$. This renders the following analysis relevant for the said experimental cases in the range $A_0 k/\nu \lesssim 100$.

Under quasiequilibrium, where $A_0 k/\nu + 1 \ll \sqrt{T_{\text{init}} k/\nu}$, Eq. (1) reduces to a nonlinear diffusion equation (see Appendix). Following an approach used by Seeger,[51] we provide an exact analytical solution of this equation in a parametric form. Let P be the solution of the following equation:

$$P\sqrt{\pi}\exp(P^2)\text{erfc}(P) = \left[1 + \frac{\nu}{A_0 k}\right]^{-1}. \tag{24}$$

Let $\lambda \geq P$ be a free parameter. Then,

$$[A] = A_0 \frac{\text{erfc}(\lambda)}{\text{erfc}(P)},$$

$$\frac{x}{2\sqrt{D_{\text{eff}} t}} = \left\{\lambda - P\exp(P^2 - \lambda^2) - \frac{\lambda}{1 + \nu/A_0 k}\left[1 - \frac{\text{erfc}(\lambda)}{\text{erfc}(P)}\right]\right\}, \tag{25}$$

where D_{eff} is an effective diffusion coefficient defined as

$$D_{\text{eff}} \equiv D(1 + A_0 k/\nu)^2/(T_{\text{init}} k/\nu). \tag{26}$$

Then,

$$[T] = T_{\text{init}} \frac{1}{1 + [A]k/\nu}, \tag{27}$$

$$[AT] = T_{\text{init}} \frac{[A]k/\nu}{1 + [A]k/\nu}. \tag{28}$$

As to the reaction rate profile $\mathbf{R}(x,t) \equiv \partial[AT]/\partial t$, we refer the reader to the Appendix for the detailed expression.

In the limiting case where $A_0 k/\nu \ll 1$, one obtains a simple expression $[A] \approx A_0 \,\text{erfc}(x/2\sqrt{D_{\text{eff}} t})$, with the effective diffusion coefficient D_{eff} then independent of A_0, namely, $D_{\text{eff}} \cong D(\nu/T_{\text{init}} k)$. In other words, the system exhibits a simple diffusion with an effective diffusion constant. This is just the approach assumed by Janson *et al.*[5] for conditions termed by them as the "high dissociation regime." It allows for a straightforward calculation of the reaction rate profile in that limit,

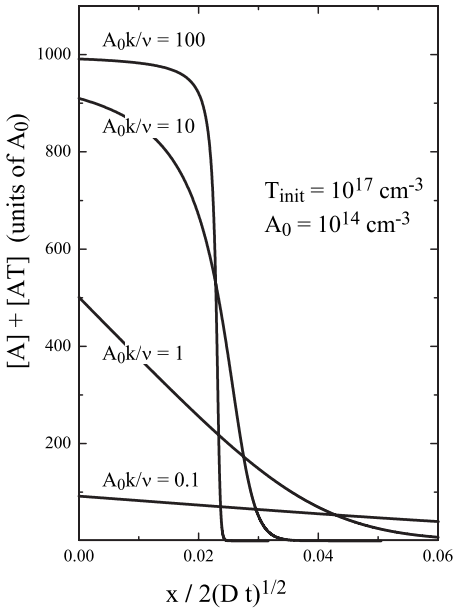

FIG. 4. Illustration of the ^{2}H ($[AT]+[A]$) concentration profile obtained by Eqs. (24)–(28), in a representative case for A_0 and T_{init} values (e.g., Ref. 5) for different values of $A_0 k/\nu$. The different shapes may correspond to different annealing temperatures that affect the $A_0 k/\nu$ value.

$$\mathbf{R}(x,t) = \frac{A_0 k}{\nu}\frac{T_{\text{init}}}{t}\frac{x}{\pi^2\sqrt{4D_{\text{eff}} t}}\exp\left(-\frac{x^2}{4D_{\text{eff}} t}\right). \tag{29}$$

Invoking the quasi steady-state assumption $\mathbf{R}(x,t) \ll k[A][T]$, one obtains the condition $t \gg \hat{t} = \nu^{-1}$ for the "sufficiently long time past the start of diffusion." Note that $\hat{t}$ attains the same value as t^* for $A_0 k/\nu \ll 1$.

To consider the opposite limiting case $A_0 k/\nu \gg 1$ (provided still that $A_0 k/\nu \ll T_{\text{init}}/A_0$), one obtains

$$[A] \approx A_0[1 - x/x_f(t)], \tag{30}$$

$$\mathbf{R}(x,t) \approx \frac{T_{\text{init}}}{2t}\left(\frac{A_0 k}{\nu}\right)^2 \frac{\alpha(1-\alpha)}{(1 + \alpha A_0 k/\nu)^3}, \tag{31}$$

where $\alpha \equiv [A]/A_0$.

A maximum (peak) of $\mathbf{R}(x,t)$ is obtained for $\alpha_{\text{peak}} \approx 0.5/[A_0 k/\nu]$; it is given by $\mathbf{R}_{\max}(t) = (2/27)(A_0 k/\nu)(T_{\text{init}}/t)$. Taking into account that $k[A][T] \approx (\nu T_{\text{init}}/3)$ at the peak position, one obtains $t^* \approx \frac{2}{9}\nu^{-1}(A_0 k/\nu)$ [see Eq. (12)].

The solution provided describes the process over a range in the $A_0 k/\nu$ parameter: $0 < A_0 k/\nu \ll T_{\text{init}}/A_0$. The upper limit of this condition is very large compared to a unity in the work of Jansen *et al.*,[5] and may as well be valid for other systems. For illustration, in Fig. 4, we show plots of $[AT]+[A]$ vs $x/2\sqrt{Dt}$ calculated profiles for different values of the

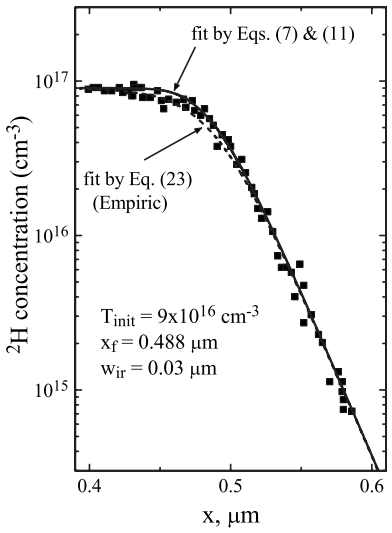

FIG. 5. Experimental concentration versus depth profile of ^{2}H in SiC, implanted and annealed at 460 °C for 30 min, after Janson *et al.* (Ref. 5) The solid line represents a theoretical fit by the irreversible reaction front expressions [Eqs. (7) and (11)]. Fit parameters are indicated in the figure.

A_0k/ν parameter, with representative A_0 and T_{init} values estimated by Jansen *et al.*[5] A well-defined down step is obtained for $A_0k/\nu \gtrsim 10$, and a standard diffusion profile is obtained for $A_0k/\nu \lesssim 1$. One may use this result for the experimental assessment of A_0k/ν by observation of the general shape of the $[AT]+[A]$ vs depth. Furthermore, a temperature change may affect the value of A_0k/ν, thus yielding changes in the general profile shapes as a function of temperature. This is another tool for obtaining the fundamental parameters governing trap-controlled diffusion of hydrogen in SiC.

VI. COMPARISON WITH EXPERIMENTAL ^{2}H PROFILE

In Fig. 5, we present a fit by our theory to experimental results by Janson *et al.* (Ref. 5, Fig. 2). The figure provides a ^{2}H depth profile in a SiC sample implanted and annealed at 460 °C for 30 min. The solid line represents a fit of the irreversible reaction front expressions to the diffusion data. The dashed line is a fit to the "empiric" equation [Eq. (23)]. Both fits provide identical fit parameters.

In the analysis of their experimental results, Janson *et al.*[5] used the tail exponential decay constant of the ^{2}H concentration profile and the initial acceptor concentration T_{init} to obtain estimates of k/D. They had to resort to a fit of a numerical solution of the differential equations to evaluate the product DA_0. To obtain an estimate of the complex dissociation frequency ν, they had to perform a new set of experiments: the ^{2}H-ion-implanted region was etched off after a certain period of diffusion, and diffusion was then let to continue. This introduced quasireversible conditions, allowing the use of a constant effective diffusion coefficient D_{eff} in solving the diffusion equations.

It should be noted that analyses of ^{2}H depth profiles such as in Fig. 5, performed after annealing for different durations, may readily yield the time dependence of x_f. On the one hand, this would allow a test of the validity of Eq. (2). On the other hand, should the said time dependence be validated, it would allow obtaining a reliable estimate of the product DA_0. Janson *et al.*[5] provided depth profiles for only two annealing durations, which are insufficient for the said purposes. Using their profiles, one may only obtain an order of magnitude estimate: $DA_0 \sim 5 \times 10^3$ cm^{-1} s^{-1}.

The method of analysis that we proposed (end of Sec. III) should save the need for resorting to numerical solutions of differential equations, as well as to interrupting the annealing for the purpose of surface etching. It requires, on the other hand, prolonged annealing periods.

VII. CONCLUSIONS

We provide a theoretical study of trap limited diffusion in solids. This study has been inspired by the experimental work on deuterium (^{2}H) diffusion in B- and Al-doped silicon carbide (SiC) performed by Janson *et al.*[5] We introduce the concept of a dynamical reaction front as a main tool of the analysis. The reaction front is a distinctive, well-defined moving zone to which the reaction is confined. The analysis provides expressions for the reaction rate profiles and spatial profiles of the mobile and postreacted (trapped) species. Under a broad range of conditions, the diffusion is accompanied by an effectively irreversible reaction at sufficiently short times and transforms into a reversible one after a characteristic time t^*. The reaction zone width is constant for short times compared to t^* but turns proportional to $\sqrt{t}$ for long times compared to t^*. We show that an experimental study of the zone-width parameter as a function of time would yield all diffusion and reaction parameters; it appears to us to be useful for quite a wide range of experimental cases.

APPENDIX: COMPLEMENTARY EXPRESSIONS

1. Definitions of the reaction zone width parameter

We use different definitions for the reaction zone-width parameter w in the irreversible and in the reversible reaction cases. For the irreversible reaction case, we define [see Eq. (7)]

$$w^2 = w_{\text{ir}}^2 \equiv \frac{\int \mathbf{R}(x,t)(x-x_f)^2 dx}{\int \mathbf{R}(x,t)dx}, \tag{A1}$$

where $\mathbf{R}(x,t)$ is the reaction rate.[8] This definition fails for the reversible reaction case; as in this case, the integral in the numerator of Eq. (A1) goes to infinity. Thus, we define w as

$$w = w_r \equiv \frac{\text{FWHM}}{4.9}, \tag{A2}$$

where FWHM is the full width at half maximum of the reaction rate profile $\mathbf{R}(x,t)$ given in Eq. (17). This expression

was chosen to render Eq. (23) appropriate for fitting to both reversible and irreversible reaction regimes.

2. Asymptotic expressions for scaling functions in the irreversible reaction case

We present some asymptotic expressions for the scaling functions for the irreversible reaction case (Sec. III) at large distance from the reaction zone.

Denoting $\xi \equiv (x-x_f)/w_{\mathrm{ir}}$, one may show that for $\xi \gg 1$,

$$S_T \cong 1,$$

$$S_A \sim S_{AT} \sim S_R \sim \exp(-1.47\xi), \tag{A3}$$

while for $\xi \ll -1$,

$$S_T \sim \exp\left[-\frac{1}{2}(1.47\xi)^2\right],$$

$$S_A \approx -\xi,$$

$$S_{AT} \approx 1 - \exp\left[-\frac{1}{2}(1.47\xi)^2\right],$$

$$S_R \approx \xi \exp\left[-\frac{1}{2}(1.47\xi)^2\right]. \tag{A4}$$

3. Asymptotic expressions for scaling functions in the reversible reaction case

We present some asymptotic expressions for the scaling functions in the reversible reaction case (Sec. IV) at large distance from the reaction zone.

Denoting $\xi_r \equiv (x-x_f)/w_r$, one may show that for $\xi_r \gg 1$,

$$S_T \cong 1,$$

$$S_A \sim S_{AT} \sim S_R \sim \exp(-\xi_r), \tag{A5}$$

while for $\xi \ll -1$,

$$Q_T \approx -1/\xi_r,$$

$$Q_A \approx -\xi_r,$$

$$Q_{AT} \approx 1 - 1/\xi_r,$$

$$Q_{\mathbf{R}} \approx 1/\xi_r^2. \tag{A6}$$

4. Derivation of the diffusion equation in Seeger's form

In the reversible reaction case, the three equations in Eq. (1) reduce into a single diffusion equation

$$\frac{\partial [A]}{\partial t}\left\{1 + \frac{T_{\mathrm{init}}k/\nu}{(1+[A]k/\nu)^2}\right\} = D\frac{\partial^2[A]}{\partial x^2}. \tag{A7}$$

For $A_0 k/\nu + 1 \ll \sqrt{T_{\mathrm{init}}k/\nu}$, one obtains

$$\left\{\frac{T_{\mathrm{init}}k/\nu}{(1+[A]k/\nu)^2}\right\}\frac{\partial [A]}{\partial t} = D\frac{\partial^2[A]}{\partial x^2}. \tag{A8}$$

Then,

$$\frac{\partial}{\partial t}\left\{\frac{-1}{(1+[A]k/\nu)}\right\} = \frac{D}{(T_{\mathrm{init}}k/\nu)}\frac{\partial^2}{\partial x^2}(1+[A]k/\nu). \tag{A9}$$

Denoting

$$U \equiv \frac{1+A_0 k/\nu}{1+[A]k/\nu}, \tag{A10}$$

one obtains the diffusion equation in Seeger's form,[51]

$$\frac{\partial U}{\partial t} = D_{\mathrm{eff}}\frac{\partial}{\partial x}\left(\frac{1}{U^2}\frac{\partial U}{\partial x}\right), \tag{A11}$$

with

$$D_{\mathrm{eff}} \equiv D\frac{(1+A_0 k/\nu)^2}{(T_{\mathrm{init}}k/\nu)}. \tag{A12}$$

5. Expression for the reaction rate

On the basis of the analytical solution given in Eqs. (24)–(28) for the reversible complex formation case, one obtains the following detailed expression for the reaction rate:

$$\mathbf{R}(x,t) = \frac{1}{t}[T]^2\frac{k[A]}{\nu T_{\mathrm{init}}\sqrt{\pi}}\frac{x}{2\sqrt{D_{\mathrm{eff}}t}}\frac{\exp(-\lambda^2)}{\mathrm{erfc}(\lambda)} \times\left\{1 + 2\lambda P\exp(P^2-\lambda^2) - \frac{1}{1+\frac{\nu}{kA_0}}\left[1 - \frac{\mathrm{erfc}(\lambda)}{\mathrm{erfc}(P)}\right] - \frac{\lambda}{1+\frac{\nu}{kA_0}}\frac{2}{\sqrt{\pi}}\frac{\exp(-\lambda^2)}{\mathrm{erfc}(P)}\right\}^{-1}. \tag{A13}$$

Equation (A13) should be used in the following manner: for each λ, calculate $[A]$, $x/2\sqrt{D_{\mathrm{eff}}t}$, and $[T]$ using Eqs. (25) and (27), then calculate $\mathbf{R}(x,t)$ using Eq. (A13).

[1] F. A. Kröger, *The Chemistry of Imperfect Crystals* (Elsevier, New York, 1974).
[2] H. Schmalzried, *Solid State Reaction* (VCH, Weinheim, 1981).
[3] H. Schmalzried, *Chemical Kinetics of Solids* (VCH, Weinheim, 1995).
[4] J. Maier, *Physical Chemistry of Ionic Materials: Ions and Electrons in Solids* (Wiley, Chichester, 2004).
[5] M. S. Janson, A. Hallén, M. K. Linnarsson, and B. G. Svensson,

Phys. Rev. B **64**, 195202 (2001).
[6] D. Ben Avraham and S. Havlin, *Diffusion and Reactions in Fractals and Disordered Systems* (Cambridge University Press, Cambridge, 2000).
[7] B. Chopard and M. Droz, *Cellular Automata Modeling of Physical Systems* (Cambridge University Press, Cambridge, 1998).
[8] L. Gálfi and Z. Rácz, Phys. Rev. A **38**, 3151 (1988).
[9] S. Cornell and M. Droz, Phys. Rev. Lett. **70**, 3824 (1993).
[10] P. L. Krapivsky, Phys. Rev. E **51**, 4774 (1995).
[11] B. P. Lee and J. Cardy, Phys. Rev. E **50**, R3287 (1994).
[12] M. Howard and J. Cardy, J. Phys. A **28**, 3599 (1995).
[13] S. J. Cornell, Phys. Rev. E **51**, 4055 (1995).
[14] G. T. Barkema, M. J. Howard, and J. L. Cardy, Phys. Rev. E **53**, R2017 (1996).
[15] Z. Jiang and C. Ebner, Phys. Rev. A **42**, 7483 (1990).
[16] Z. Koza, Physica A **240**, 622 (1997).
[17] B. Chopard, M. Droz, T. Karapiperis, and Z. Racz, Phys. Rev. E **47**, R40 (1993).
[18] M. Sinder and J. Pelleg, Phys. Rev. E **60**, R6259 (1999).
[19] M. Sinder and J. Pelleg, Phys. Rev. E **61**, 4935 (2000).
[20] M. Sinder and J. Pelleg, Phys. Rev. E **62**, 3340 (2000).
[21] Z. Koza, Phys. Rev. E **66**, 011103 (2002).
[22] Z. Koza, Eur. Phys. J. B **32**, 507 (2003).
[23] Z. Koza, Physica A **330**, 160 (2003).
[24] H. Taitelbaum, S. Havlin, J. E. Kiefer, B. Trus, and G. H. Weiss, J. Stat. Phys. **65**, 873 (1991).
[25] E. Ben-Naim and S. Redner, J. Phys. A **25**, L575 (1992).
[26] Z. Koza and H. Taitelbaum, Phys. Rev. E **54**, R1040 (1996).
[27] Z. Koza, J. Stat. Phys. **85**, 179 (1996).
[28] M. A. Rodriguez and H. S. Wio, Phys. Rev. E **56**, 1724 (1997).
[29] M. Z. Bazant and H. A. Stone, Physica D **147**, 95 (2000).
[30] J. Magnin, Eur. Phys. J. B **17**, 673 (2000).
[31] T. Unger and Z. Rácz, Phys. Rev. E **61**, 3583 (2000).
[32] S. M. Cox and M. D. Finn, Phys. Rev. E **63**, 051102 (2001).
[33] M. Sinder and J. Pelleg, Phys. Rev. E **65**, 060101(R) (2002).
[34] M. Sinder, Phys. Rev. E **65**, 037104 (2002).
[35] B. M. Shipilevsky, Phys. Rev. E **67**, 060101(R) (2003).
[36] M. Sinder, J. Pelleg, V. Sokolovsky, and V. Meerovich, Phys. Rev. E **68**, 022101 (2003).
[37] P. Polanowski and Z. Koza, Phys. Rev. E **74**, 036103 (2006).
[38] Y.-E. L. Koo and R. Kopelman, J. Stat. Phys. **65**, 893 (1991).
[39] H. Taitelbaum, Y.-E. Lee Koo, S. Havlin, R. Kopelman, and G. H. Weiss, Phys. Rev. A **46**, 2151 (1992).
[40] A. Yen, Y.-E. Lee Koo, and R. Kopelman, Phys. Rev. E **54**, 2447 (1996).
[41] H. Taitelbaum, B. Vilensky, A. Lin, A. Yen, Y.-E. Lee Koo, and R. Kopelman, Phys. Rev. Lett. **77**, 1640 (1996).
[42] S. H. Park, S. Parus, R. Kopelman, and H. Taitelbaum, Phys. Rev. E **64**, 055102(R) (2001).
[43] C. Leger, F. Argoul, and M. Z. Bazant, J. Phys. Chem. B **103**, 5841 (1999).
[44] C. N. Baroud, F. Okkels, L. Ménétrier, and P. Tabeling, Phys. Rev. E **67**, 060104(R) (2003).
[45] M. Haque, Phys. Rev. E **73**, 066207 (2006).
[46] E. Mollvo, Ann. Phys. **29**, 5 (1937).
[47] F. N. Rhines, W. A. Johnson, and W. A. Andersen, Trans. AIME **147**, 205 (1942).
[48] I. Bloem and F. A. Kroger, Philips Res. Rep. **12**, 281 (1957).
[49] G. Astarita, *Mass Transfer with Chemical Reactions* (Elsevier, Amsterdam, 1967).
[50] D. A. Frank-Kamenetsy, *Diffusion and Heat Transfer in Chemical Kinetics* (Plenum, New York, 1969).
[51] A. Seeger, Phys. Status Solidi A **61**, 521 (1980).